Latin American Journal of Solids and Structures
www.lajss.org

Progressive failure prediction of pinned joint in quasi-isotropic laminates used in pipelines

Abstract

To simulate the progressive failure of pinned joint in quasi-isotropic [0/45/-45/90]s glass fiber reinforced polymer (GFRP) composite laminates used in pipeline, 3-D finite element model is employed in the present work. Hashin failure criterion as a progressive damage model associated with Virtual-Crack-Closing-Technique (VCCT) delamination model has been adopted to predicate the failure due to fiber breakage, matrix cracking and delamination in composite pinned joint. This technique may be an innovation for this paper. *W/D* has been changed to get different modes of failure, i.e. tension, shear-out and bearing failures, in composite pinned joint,. The failure mode for GFRP composite pinned joint has been predicted finally after prediction the failure at each ply laminate of stacking sequence [0/45/-45/90]s. An experimental work of pinned joint in quasi-isotropic GFRP composite laminates has been conducted to validate the present numerical results. The numerical and experimental results showed an agreement between them. Therefore, the present 3D finite element model can be considered as a good candidate to expect the progressive damage in composite pinned joints.

Keywords

Composite pinned joint, quasi-isotropic glass fiber reinforced polymer, 3-D finite element analysis, Hashin failure criteria, Virtual-Crack-Closing-Technique, delamination damage model.

A.A. Abd-Elhady[a]
M.A. Mubaraki[b]
H.E.M Sallam[c]*

[a]Mechanical Engineering Department., Jazan University, Jazan, KSA; on sabbatical leave from Mechanical Design Department, Mataria, Helwan University, Cairo, Egypt. E-mail: aaa_elhady@yahoo.com

[b] Civil Engineering Department, Jazan University, Jazan, KSA. E-mail: almustkshef@hotmail.com

[c] Civil Engineering Department, Jazan University, Jazan, KSA; on sabbatical leave from Materials Engineering Department, Zagazig University, Zagazig, Egypt. E-mail: hem_sallam@yahoo.com

*Corresponding author

http://dx.doi.org/10.1590/1679-78255061

Received: May 04, 2018
In Revised Form: May 14, 2018
Accepted: May 28, 2018
Available Online: May 29, 2018

1 INTRODUCTION

Polymeric composite pipelines are increasingly used for a variety of applications, such as in the oil, gas and high pressure container industries. As is already known, the composite adhesive/bolted joints are potentially sources of weakness and additional weight in engineering structures and mechanical components, El-Emam et al. (2016, 2017); El-Sisi et al. (2014); Sallam et al. (2011). The stress concentrations due to the presence of the fastener hole cause delamination or other types of damage modes and final failure, Sallam et al. (2011).. Intra-laminar damage (matrix cracking and tension/compression fiber breakage) and delamination damage (inter-laminar damage) are the main types of damages in composite structures. Progressive damage models (PDMs) focus on failure criterion and the material degradation rule, Hashin (1980. Several researchers, El-Sisi et al. (2015); Zhou et al. (2013); McCarthy et al. (2005), used Hashin failure criterion (Hashin 1980) to analysis the damage in pinned joints made of composite materials.

Abd-Elhady and Sallam (2015) used a different approach than progressive damage model PDM to expect the type of failure in pinned joint. Abd-Elhady and Sallam (2015) studied the mode of failure and ultimate strength of pinned joined due to the existence of scratch like a crack at the pin hole surface. Khashaba at al. (2006) showed that, damage initiated firstly by delamination between the ±45°, and 90o layers, secondly the layers of 90o were failed by net tension failure mode, finally catastrophic failure were produced for ±45° layers. The delamination can initiate in a shearing mode. On the other hand, through thickness cracks and delamination may be occurred during the bearing mode of failure. The integrity of composite structures may be vanished by delamination and subsequently severely lose their strength. Furthermore, the delaminations are difficult to detect experimentally. Nassar et al. (2007) used microscopically experimental technique to study the effect clamping force on the occurrence of delamination. Therefore, 3D finite

element analysis may be a good candidate to predict the failure mode of composite bolted joints taking into its consideration delamination effects.

1.1. Problem description

The main objective of the present work is to build a progressive damage model based on Hashin failure criterion associated with Virtual-Crack-Closing-Technique (VCCT) delamination model to study of the initiation and progressive damage of pinned connections in quasi-isotropic GFRP composite laminates. The effect of pinned joint geometry is considered in this work. To validate the present numerical results, the experimental work has been conducted with different joint geometry to achieve different modes of failure.

2. FINITE ELEMENT MODEL

The mechanical properties of GFRP lamina used in the present investigation are shown in Table 1, which is extracted from the authors' previous work, Abd-Elhady and Sallam (2015); Sallam and Abd-Elhady (2015); Ghanem et al. (2006). Eight quasi-isotropic laminates with [0/45/-45/90]s lay-ups are simulated with continuum shell elements type (SC8R). Table 1 states the material properties of GFRP used in the present work. The dimensions of GFRP Composite plate with fastener hole and the bolt geometry are listed in Table 2. In order to simulate the progressive damage for different mode of failure, *W/D* has been changed to obtain tension failure, shear out failure and bearing failure as shown in Fig. 1. In the present work, a thin epoxy interface layer with thickness 0.1 mm was used to predict a 3-D delamination effects between the plies and simulated using Linear 8-node hexahedral brick elements (C3D8R). It was simulated as isotropic material with modulus elasticity 4 GPa and Poisson's ratio 0.398 (Warren et al. 2016). The interface layer was tie at each face of GFRP lamina.

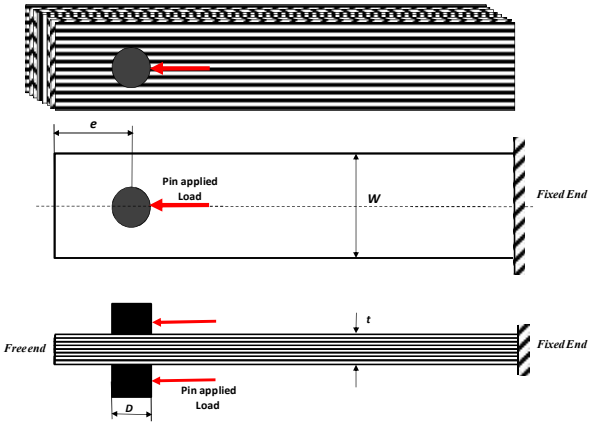

Figure 1: *Schematic of quasi-isotropic GFRP composite laminates Pinned joints configuration with eight composite layers [0/45/-45/90]s used in present study*

Table 1: *Material properties and strength data of GFRP lamina composite material Abd-Elhady and Sallam (2015)*

Symbol	value	Property
E_{11}	32	Young's modulus in fiber direction (GPa)
E_{22}	7	Young's modulus in the transverse direction (GPa) (In *Y* direction)
E_{33}	7	Young's modulus in the transverse direction (GPa) (In *Z* direction)
G_{12}	2.56	In- plane shear modulus (GPa) (*X-Y* plan)
G_{13}	1.8	In- plane shear modulus (GPa) (*X-Z* plan)
G_{23}	1.8	In- plane shear modulus (GPa) (*Y-Z* plan)
v_{12}	0.27	Poisson's Ratio (X-Y plan)
v_{13}	0.25	Poisson's Ratio (*X-Z* plan)
v_{23}	0.25	Poisson's Ratio (*Y-Z* plan)
X^T	174	denotes the longitudinal tensile strength (MPa)
X^C	135	denotes the longitudinal compressive strength (MPa)
Y^T	20	denotes the transverse tensile strength (MPa)
Y^C	35	denotes the transverse compressive strength (MPa)
S^L	124	denotes the longitudinal shear strength (MPa)
S^T	124	denotes the transverse shear strength (MPa)
α	0	a coefficient that determines the contribution of the shear stress to the fiber tensile initia-

tion criterion (Barbero et al. 2013)

Table 2: *GFRP composite plate with fastener hole and bolt geometry*

Symbol	Value	Description
L	100	Laminate length (mm)
D	6.2	Fastener hole and bolt shank diameter (mm)
T	0.5	Lamina thickness (mm)
W/D	2, 3, 4, and 5	Plate width over fastener hole diameter
e	18.6	The distance between the center of the fastener hole and plate free end (mm)
D_{bo}	10	Outer diameter of the bolt head and nut (mm)

The steel bolts were simulated as isotropic material, with modulus of elasticity 207 GPa and Poisson's ratio 0.3 and meshed using C3D8R. The clearance between the bolt shank and fastener hole is assumed to be zero. The outer diameter, D_{bo}, of the bolt head and nut was kept constant equal 10 mm. Contact pairs were defined between interacting surfaces of the parts. The interaction between the bolt and composite laminates was simulated using "Surface to surface contact". Progressive failure analyses through the finite element models were performed using the commercial finite element software ABAQUS (2016). Mesh of the pinned joint assembly is shown in Fig 2.

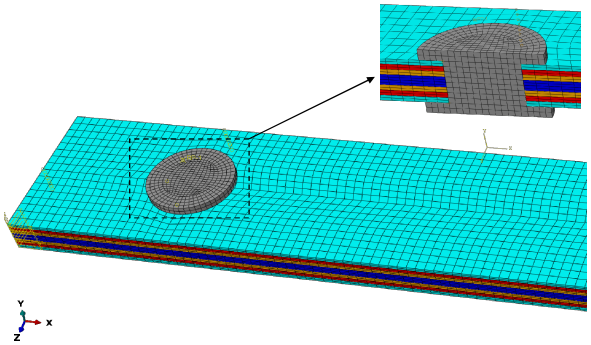

Figure 2: *Mesh of the pinned joint assembly.*

2.1 Progressive damage model

Hashin failure criterion as a progressive damage model associated with VCCT delamination model is suggested in the present work to predicate the damages in fiber and matrix damage in addition to the delamination damage in quasi-isotropic [0/45/-45/90]s GFRP composite pinned joint. This technique may be an innovation for this paper.

2.1.1 Hashin failure criterion

The 3-D damage model using ABAQUS code (ABAQUS 2016) is implemented in this paper to predict the modes of intra-laminar damage based on Hashin's theory (Hashin 1980; Hashin and Rotem 1973). Hashin failure criteria are considering four different failure modes: fiber tension, fiber compression, matrix tension and matrix compression. Moreover, it considers that the behavior of the undamaged material is linearly elastic. The procedure steps of the present Hashin model are described well elsewhere (ABAQUS 2016; Barbero et al. 2013; Hashin and Rotem 1973). The initiation criteria have the following general forms:

1- Fiber tension ($\sigma_{11} \geq 0$):

$$F_f^t = \left(\frac{\sigma_{11}}{X^T}\right)^2 + \alpha\left(\frac{\tau_{12}}{S^L}\right)^2 \tag{1}$$

2- Fiber compression ($\sigma_{11} < 0$):

$$F_f^c = \left(\frac{\sigma_{11}}{X^C}\right)^2 \tag{2}$$

3- Matrix tension ($\sigma_{22} \geq 0$):

$$F_m^t = \left(\frac{\sigma_{22}}{Y^T}\right)^2 + \left(\frac{\tau_{12}}{S^L}\right)^2 \tag{3}$$

4- Matrix compression ($\sigma_{22} < 0$):

$$F_m^c = \left(\frac{\sigma_{22}}{2S^T}\right)^2 + \left[\left(\frac{Y^C}{2S^T}\right)^2 - 1\right]\frac{\sigma_{22}}{Y^C} + \left(\frac{\tau_{12}}{S^L}\right)^2 \tag{4}$$

where σ_{ij} are the scalar components of stress tensor where: *i,j* = 1-3, *X* and *Y* are the strengths in the fiber direction and transverse direction, respectively, *α* is a coefficient that determines the contribution of the shear stress to the fiber tensile initiation criterion, and *S* is the shear allowable. The subscripts '*c*' and '*t*' denote compression and tension. The strength data of GFRP composite materials used in the present model are given in table 1. Damage occurs when value of one of the above initiation criterion reaches the unity or greater than it. Therefore, the value of each initiation criterion in each step of loading has been traced to identify the stages of the progressive failure.

2.1.2 Delamination Bonding Model

The energy release rate, G, considered one of the main fracture parameter can predict the crack growth under different mode of mixity. Therefore, several researchers (Krueger 2004; Liu et al. 2011; Xie and Biggers 2006; Zeng et al. 2016) utilized the VCCT to get the energy release rate, *G*, to determine the delamination in composite laminates. The main assumption of VCCT is that the strain energy released required for the crack propagation length *Δa* is equal to that for closing two separate crack surface with crack length *Δa* (ABAQUS 2016)as shown in Fig. 3. Figure 3 illustrates the crack propagation between composite layers from *i* to *j*: (a) before propagation and (b) after propagation.The crack tip nodes (2 and 5) will be separated when the value of equivalent mode I, II, III energy release rate, G_{equiv}, is equal to or greater than the equivalent critical energy release rate, G_{equivC}, value as follows:

$$\frac{G_{equiv}}{G_{equivC}} \geq 1.0 \tag{5}$$

In the present work, B-K law (Benzeggagh and Kenane 1996) has been adopted to compute the value of G_{equivC} as follows:

$$G_{equivC} = G_{IC} + \left(G_{IIC} - G_{IC}\right)\left(\frac{G_{II} + G_{III}}{G_I + G_{II} + G_{III}}\right)^{\eta} \tag{6}$$

where:

$$G_I = \frac{u_{1,6} F_{u,2,5}}{2\Delta a b} \tag{7}$$

$$G_{II} = \frac{v_{1,6} F_{v,2,5}}{2\Delta a b} \tag{8}$$

$$G_{III} = \frac{w_{1,6} F_{w,2,5}}{2\Delta a b} \tag{9}$$

where G_I, G_{II}, and G_{III} are Mode I, Mode II, and Mode III of the energy release rate, respectively. G_{IC} and G_{IIC} are the critical values of Mode I and Mode II energy release rates, respectively. b is the plate width. The mixed mode ratio is determined by the parameter η, η ∈ (1.0 − 2.0) (ABAQUS 2016). “Node to surface contact” is adopted to simulate the interaction type between the interfaces layers, while, “VCCT” failure criteria is adopted to simulate the bonding property between the two interface surfaces.

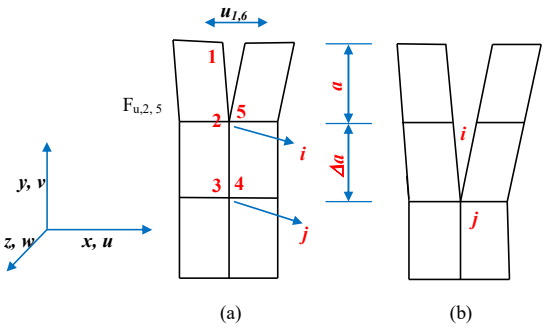

Figure 3: *Schematic representation of crack propagation between composite layers: (a) before propagation and (b) after propagation.*

3 NUMERICAL RESULTS

Fig. 4 shows the effect of *W/D* on the progressive damage failure of the pinned joint in quasi-isotropic [0/45/-45/90]s GFRP composite laminates. The final damage mode changed from net-tension mode of failure at *W/D* = 2 and 3 to bearing mode of failure which converts to shear-out mode of failure along beneath the fastener hole due to the pressure from the bolt at *W/D* = 4 and 5. The fiber compression damage area increases by increasing the value of *W/D* and it appears at the bearing zone. However, the value of fiber tension damage decreases by increasing the value of *W/D*. On the other hand, the matrix compression damage area decreases by increasing the value of *W/D* and it appears at the net-tension zone, while, the matrix tension damage area increases by increasing the value of *W/D* shown and it appears at bearing zone, as shown in figure 4. Generally, the compressive failure of fiber associated with tensile failure of matrix is detected at the bearing damage zone and the area of this zone increased by increasing *W/D*, while, the tensile failure of fiber associated with compressive failure of matrix is detected at net-tension damage zone and the area of this zone decreased by increasing the value of *W/D*.

In order to predict the stages of progressive failure of quasi-isotropic composite pinned joint, the failure at each ply lamina of stacking sequence [0/45/-45/90]s was traced firstly. Figures 5 and 6 show the damage area of each ply laminate with stacking sequence [0/45/-45/90]s for *W/D* = 2 and 5 respectively. As mentioned before in Fig. 4, the final failure of *W/D* = 2 and 3 are net tension while for *W/D* = 4 and 5 are shear out.

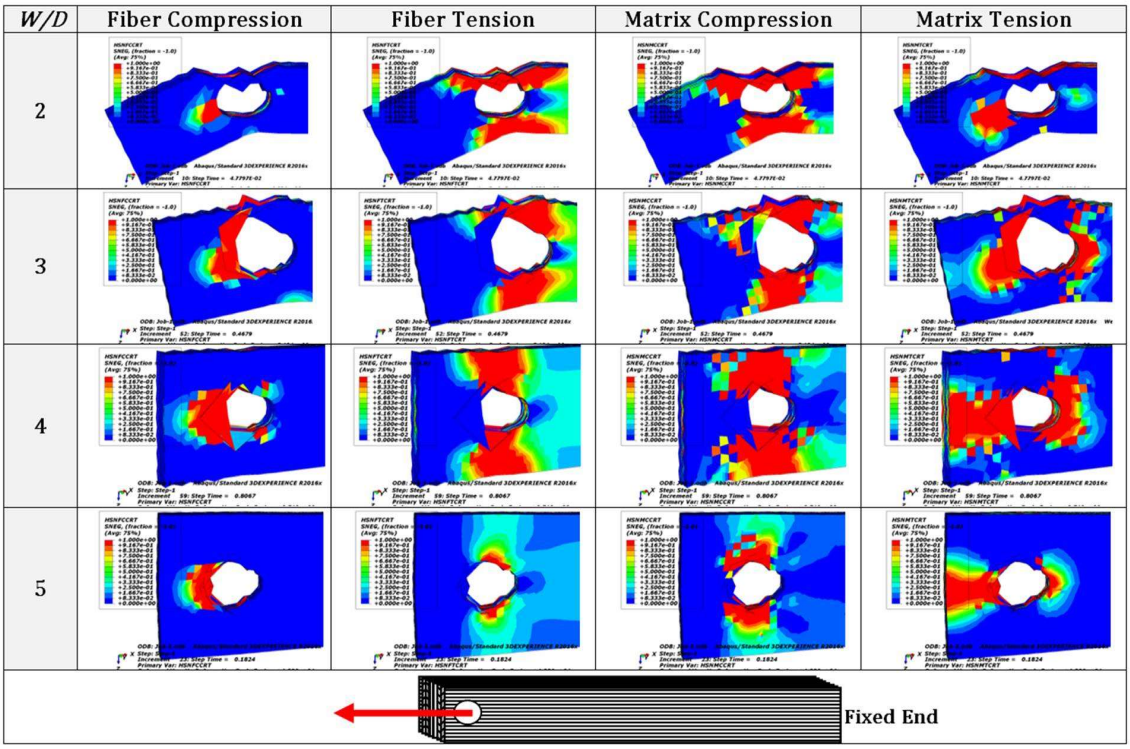

Figure 4: *Progressive damage failure of the pinned joints structure made of GFRP laminate with stacking sequence [0°/45°/-45°/90°]s for different W/D.*

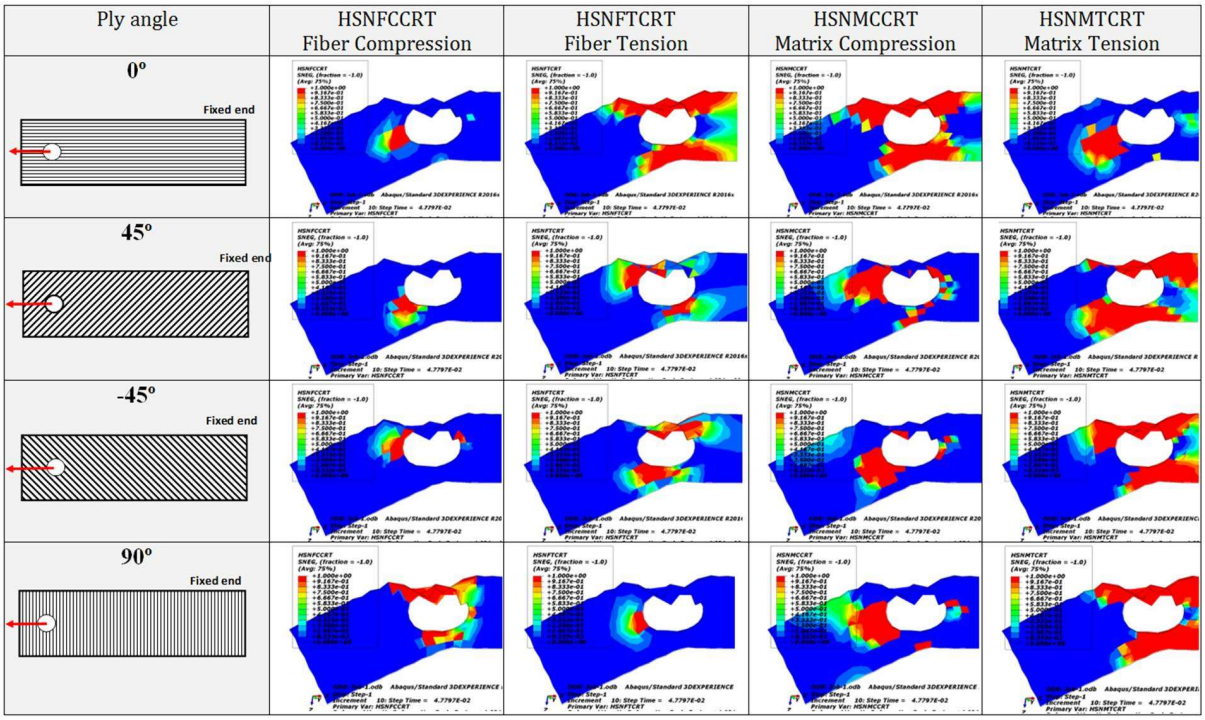

Figure 5: *Progressive damage failure of first four layer for the final failure of the pinned joints structure made of GFRP laminate with stacking sequence[0°/45°/-45°/90°]s for different W/D = 2.*

It can be seen from figures 5 and 6 that, the site of tensile/compressive damage of the fiber depends on the direction of the fiber in each lamina, i.e. the site of compressive failure of fibers in 0o ply is found at bearing damage zone, while, it is found at net-tension damage zone for 90o ply. The same observation is found for tensile failure of fibers but in the opposite sites, as shown in Figs 5 and 6. In general, the tensile failure of fibers is associated with compressive failure of matrix, while, the compressive failure of fibers is associated with tensile failure of matrix.

It can be seen from Fig. 5, at the site of net-tension failure the largest size of fiber tension damage zone is found in 0° ply, while, the largest size of matrix tension damage zone is found in 90° ply. Furthermore, the size of contact damage between the bolt and the hole is very small in all plies. The damage at the net-tension zone is larger than that at bearing zone. Therefore, the mode of the pinned composite joint with stacking sequence $[0/45/-45/90]_s$ with *W/D*= 2 is a net-tension mode of failure. On the other hand, the size of fiber tension damage zone is very small in all plies for *W/D* = 5, as shown in Fig. 6. The dominate type of failure is matrix tension followed by matrix compression. In the two paths of shear out mode of failure in ±45° plies, one path in +45° ply failed due to matrix tension and the other failed due to matrix compression vice versa with -45° ply. Therefore, the mode of failure the pinned composite joint with *W/D* = 5 is a shearing mode.

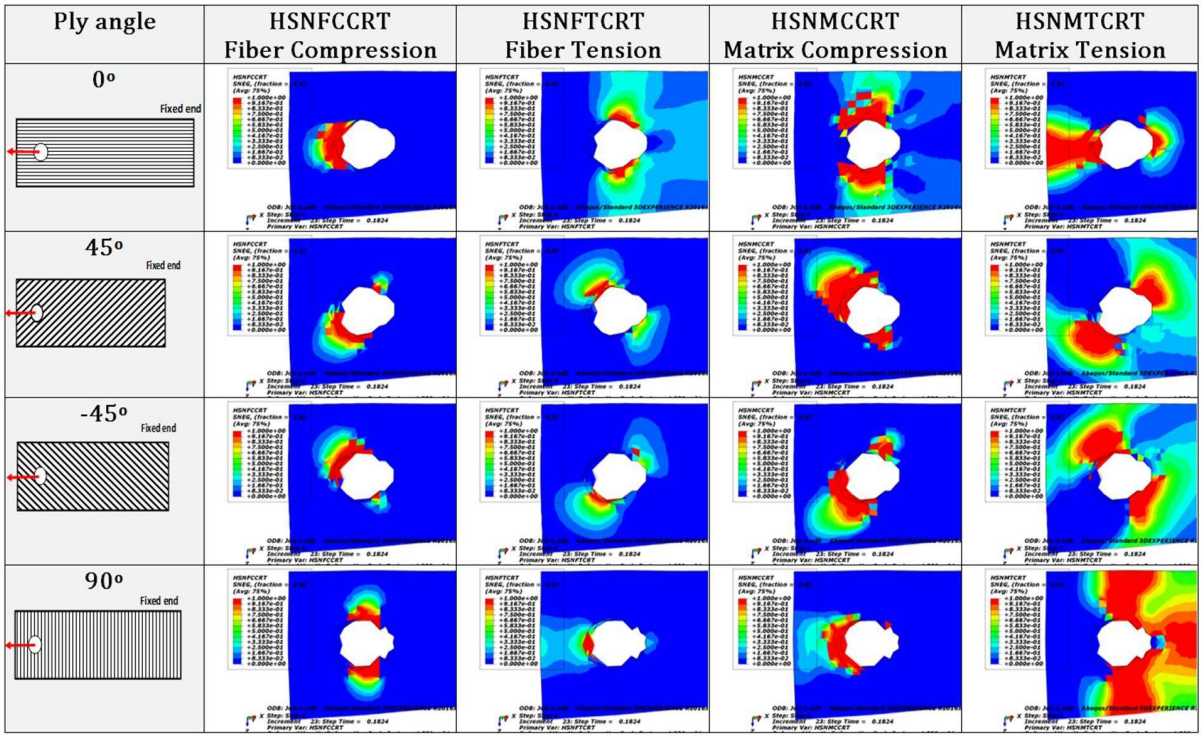

Figure 6: *Progressive damage failure of first four layer for the final failure of the pinned joints structure made of GFRP laminate with stacking sequencesequence [0°/45°/-45°/90°]s for different W/D= 5.*

Tables 3 and 4 illustrate the relationship between constituent failure mechanism of different plies laminates of pinned joints structure from initial to final failure and the pin displacement for *W/D*= 2 and 5 respectively. Table 3 and 4 depict that the failure of the pinned joint commenced from the matrix damage for all plies and then the damage extended to the fibers. For *W/D* = 2, the fibers damage starts from 0° ply followed ±45° plies and finally to 90° ply, see Table 3. However for *W/D* = 5, at the beginning the matrix failed in compression followed failure matrix tension in all plies with fiber compression failure in 0° ply. The same sequence of fiber compression failure in different plies is found in *W/D* = 5, i.e. started in 0° ply and finally in 90° ply. The fiber tension failure started from the ±45° plies and then to the 0° and 90° plies at the same time, see Table 4. For *W/D* = 2 the damage began at load-displacement = 0.025 mm before the damage of *W/D*= 5 starting at load-displacement = 0.05 mm, while, the final failure load of *W/D* = 2 is reached at load-displacement = 0.12 mm and it is lower than that of *W/D*= 5 (reached at load-displacement = 0.29 mm).

Table 3: *Constituents failure modes from initial to final failure of bolted joints structure made of GFRP laminate with stacking sequence [0°/±45°/90°]s of W/D = 2.*

Load Pin disp. (mm)	0 degree layer				45 degree layer				-45 degree layer				90 degree layer			
	Fiber		Matrix		Fiber		Matrix		Fiber		Matrix		Fiber		Matrix	
	C	T	C	T	C	T	C	T	C	T	C	T	C	T	C	T
0.025			•	•			•	•			•	•			•	•
0.044	•	•	•	•			•	•	•		•	•			•	•
0.072	•	•	•	•	•	•	•	•	•	•	•	•			•	•
0.12	•	•	•	•	•	•	•	•	•	•	•	•	•	•	•	•

Note: • mean damage, C: mean compression damage and T: mean tension damage

Table 4: *Constituents failure modes from initial to final failure of bolted joints structure made of GFRP laminate with stacking sequence [0°/±45°/90°]s of W/D = 5.*

Load Pin disp. (mm)	0 degree layer				45 degree layer				-45 degree layer				90 degree layer			
	Fiber		Matrix		Fiber		Matrix		Fiber		Matrix		Fiber		Matrix	
	C	T	C	T	C	T	C	T	C	T	C	T	C	T	C	T
0.05			•				•				•				•	
0.1	•		•	•			•	•	•		•	•			•	•
0.175	•		•	•	•	•	•	•	•	•	•	•			•	•
0.29	•	•	•	•	•	•	•	•	•	•	•	•	•	•	•	•

Note: • mean damage, C: mean compression damage and T: mean tension damage

4 Experimental Verification

The experimental work conducted by Ghanem et al (2006) was recall in the present work to validate the applicability of 3D finite element method for simulating the progressive damage in composite pinned joint. Quasi-isotropic $[0/45/-45/90]_s$ glass fiber reinforced epoxy (GFRE) composite laminates with 4±0.1 mm thickness were made using prepregs method. The average value of fiber volume fraction (V_f) was 39%. A series of mechanical tests were carried out using a universal testing machine with machine crosshead speed during all tests was 0.1 mm/min. The number of specimens, tests procedures and specifications are described in details elsewhere, Ghanem et al (2006). Table 5 states the mechanical properties of the quasi-isotropic $[0/45/-45/90]_s$ GFRE composite laminates which are the average values of five specimens in each test. The dimensions of pinned joint quasi-isotropic laminates specimens have the same dimensions used in the numerical work, see table 2.

Table 5: *Mechanical properties of quasi-isotropic [0/±45/90]s.*

UTS, MPa	E, GPa	Shear Stress, MPa	Compressive Stress, MPa	Flexural Stress, MPa	P/Δ, kN/mm
181	18	140	196	**215**	**5**

5 COMPARISONS BETWEEN NUMERICAL AND EXPERIMENTAL RESULTS

The comparisons between the numerical predictions and the experimental results for final failure of composite pinned joints with *W/D* = 2 and 5 are shown in Figs. 7 and 8 respectively. In the case of *W/D* = 2, it is found experimentally that, the failure of fiber and matrix in addition to the delamination appeared at the root of the fastener hole as a net-tension mode of failure, Fig. 7.a. This observation is compatible with the fiber tension damage predicted numerically at the same site, Fig. 7.b. It can be observed from figure 8.a, the fiber and matrix fracture appeared as shear out mode of failure, as well as the material is moved away the contact region by the bearing stress to produce the shear out fracture. It can be seen that the fiber tension damage and matrix compression damage appear at the root of the fastener hole and it are very small compared to the fiber compression damage and matrix tension damage which appears at the contact area between the fastener hole and bolt.

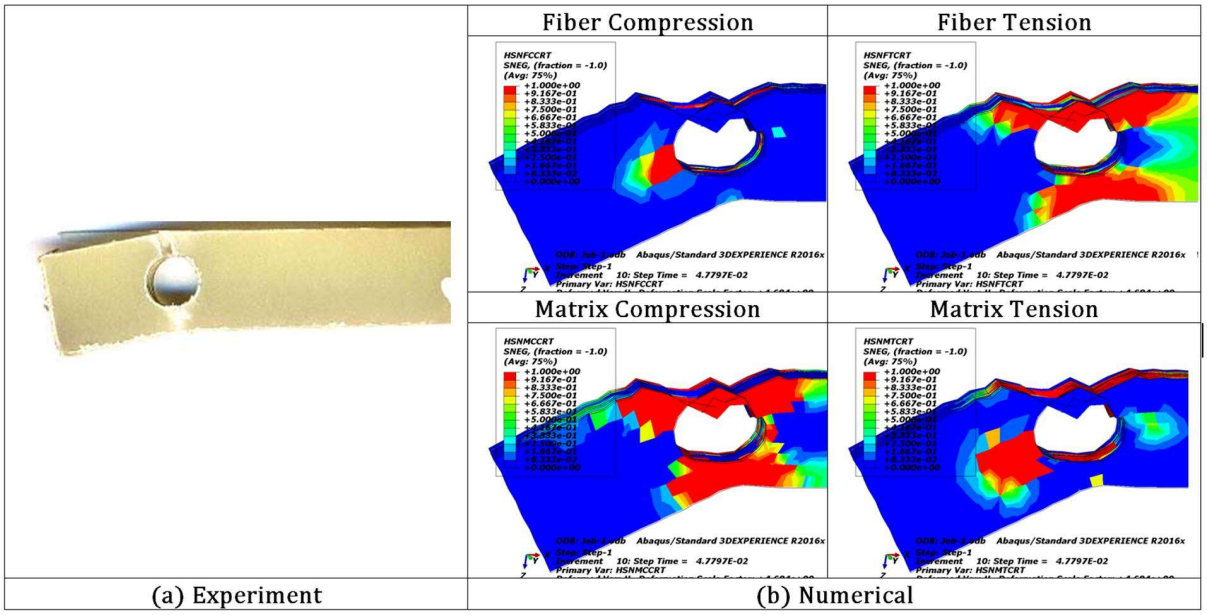

Figure 7: *Damage observed after final failure for pin load of GFRP composite joint test for W/D = 2.*

Generally, there is an agreement between the numerical predictions and the experimental results, where the net-tension mode of failure is observed in the case of *W/D* = 2 and shear out mode of failure is observed in the case of *W/D* = 5 for both of them as shown in Figs 7 and 8. Therefore, it can be concluded that the present finite element analysis can be considered as a good candidate to predict the failure mode of pinned joint in quasi-isotropic $[0/45/-45/90]_S$ glass fiber reinforced polymer (GFRP) composite laminates.

A comparison between Hashin model associated with delamination model using VCCT and Hashin model only through evaluating their predictions of mode of failure composite pinned joints and the load-pin displacement curves to those measured experimentally. Figure 9.a shows the mode of failure mode observed experimentally for different values of *W/D*. it is clear that, the damage consists of (1) fiber damage, (2) matrix damage and (3) delamination damage between the layers. Fig. 9.b illustrates the numerical results of final failure based on Hashin model associated with delamination model. This model covers the three types of the above damages. It can be seen from the figure 9.b the final failure mode changes from net-tension mode at *W/D* = 2 and 3 to shear out mode at *W/D* = 4 and 5. This indicates that the numerical results of Fig 9.b are in good agreement with the experimental results. However, Fig. 9.c shows the numerical results based on Hashin model only. Hashin model presents only two types of damage, namely (1) fiber damage (tension or compression) and (2) matrix damage (tension or compression). This means that, Hashin model is applicable only for single layer composite and it is not appropriate for laminated composite.

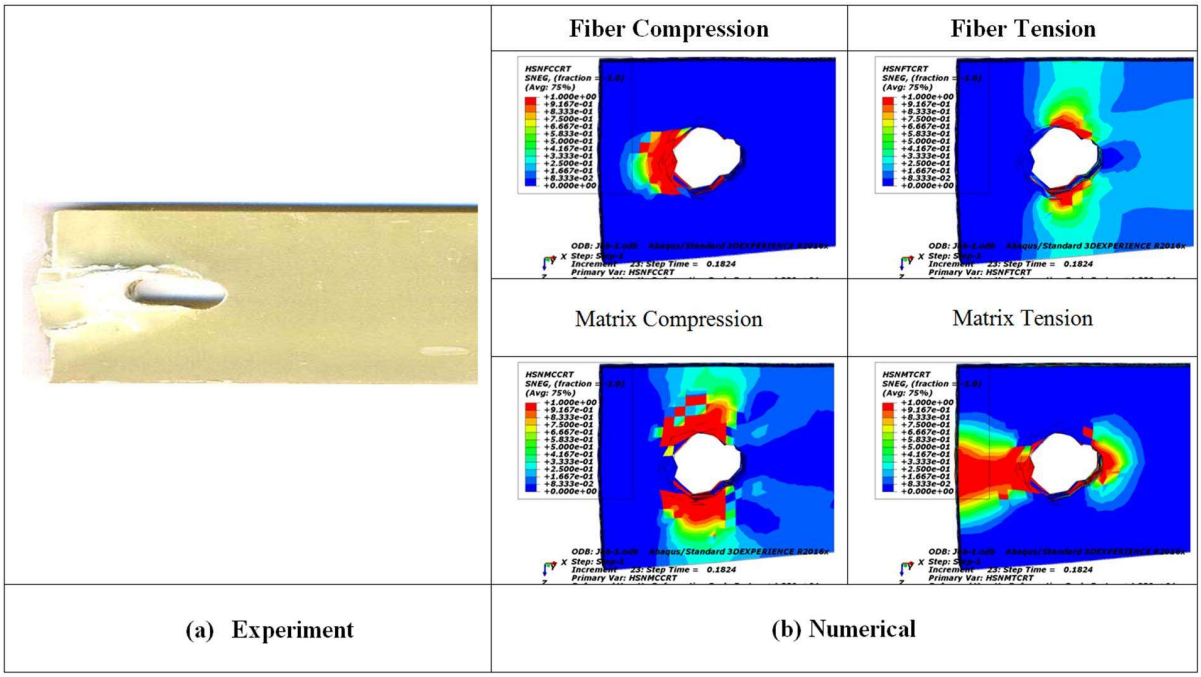

Figure 8: *Damage observed after final failure for pin load of GFRP composite joint test for W/D = 5.*

Fig. 10 shows the load-pin displacement curves obtained from the numerical damage models, i.e. Hashin model (dash line) and Hashin model associate with delamination model (solid line), and the experiment results (red line) for different values of *W/D*. For all values of *W/D*, there is a good agreement between the load–displacement curve predicted from Hashin associated delamination model and those measured from the experimental work. However, Hashin model failed to predict the descending part of the curve. For *W/D* = 2 and 3, a brittle failure of pinned joint is observed, i.e. sudden drop in the strength after reaching its ultimate strength. For *W/D* = 4 and 5, a ductile failure of pinned joint is observed, i.e. the bearing failure occurred at load equals about 3.5 kN and pin-displacement equals 0.3 mm (starting of the shear-out failure). After that, the shear-out damage increase associated with increasing the resistance of the pinned joint to reach its ultimate strength at the final stage of the shear-out damage (Load ≈ 4.5 kN and pin-displacement ≈ 0.6 mm). This means the pin-displacement at the final stage of the shear-out damage is two times that at the commencement of the shear-out damage and the load ratio equals 4.5/3.5 ≈ 1.25.

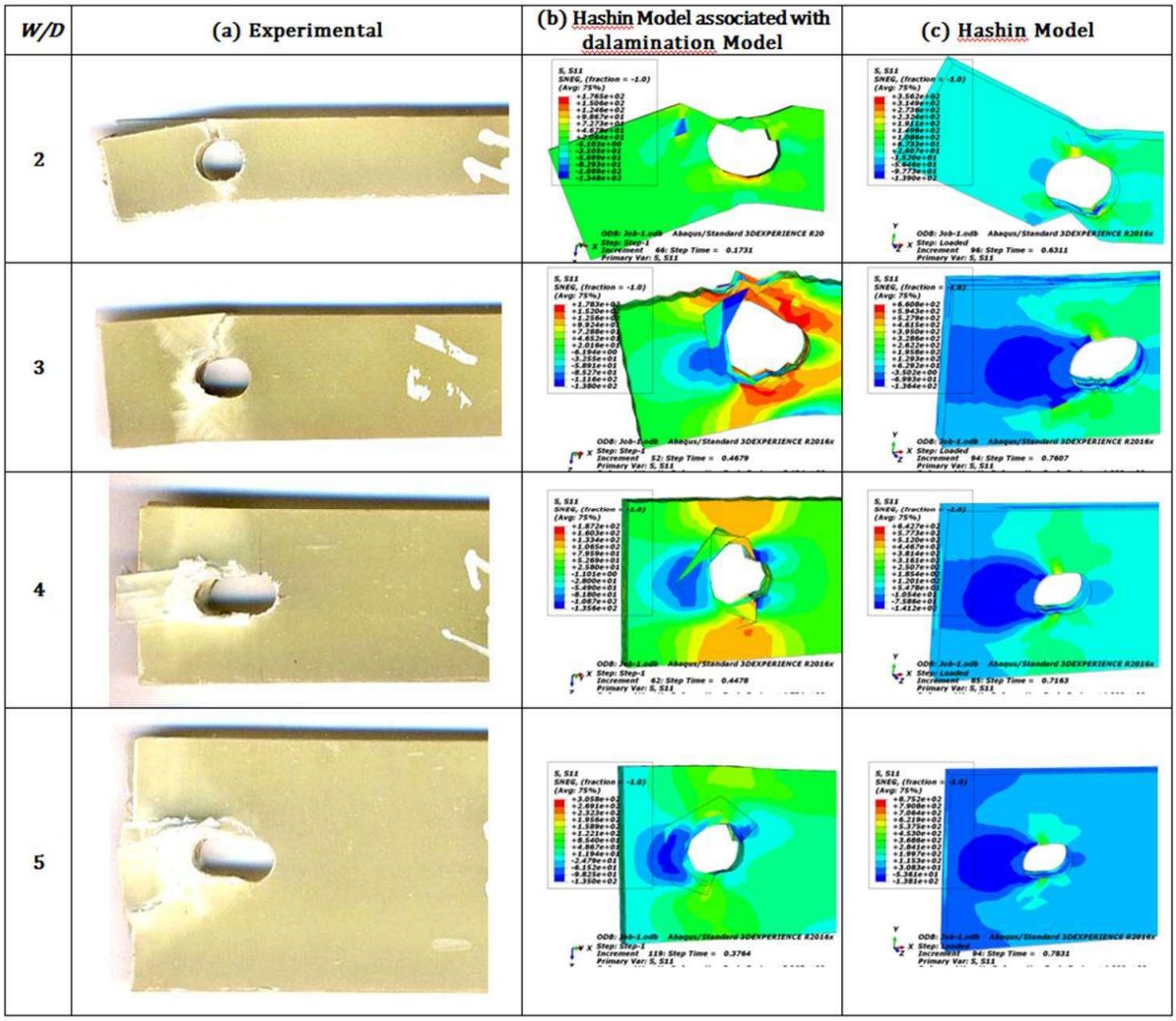

Figure 9: *Comparison between (a) the experimental final failure and (b) Hashin model associated with delamination model (using VCCT) and (c) Hashin model, for different W/D*

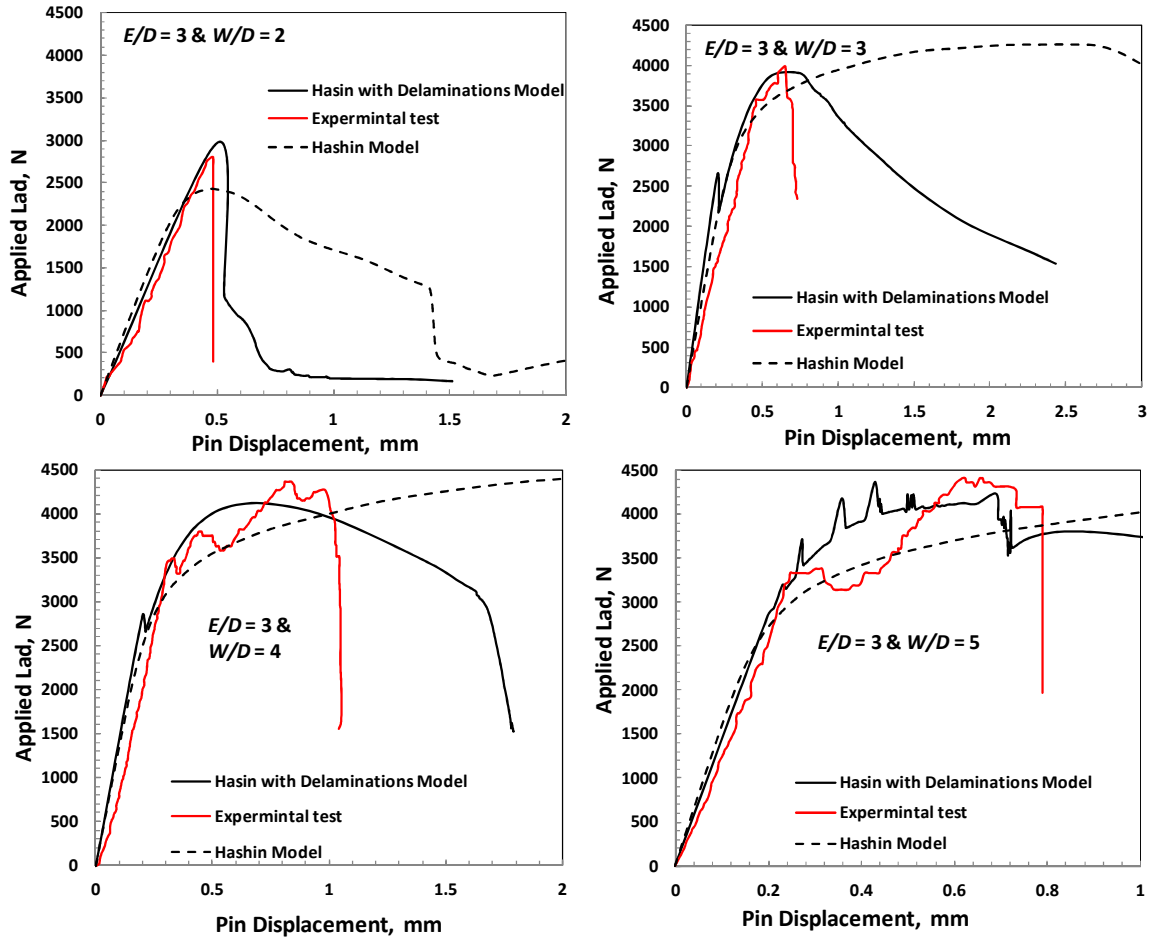

Figure 10: *Comparison between experimental results and the predicted values*

6 CONCLUSIONS

Based on the above results, the following conclusions can be drawn:

1- The compressive failure of fiber associated with tensile failure of matrix is detected at the bearing damage zone and the area of this zone increased by increasing *W/D*.

2- The tensile failure of fiber associated with compressive failure of matrix is detected at net-tension damage zone and the area of this zone decreased by increasing the value of *W/D*.

3- The site of tensile/compressive damage of the fiber depends on the direction of the fiber in each lamina, i.e. the site of compressive failure of fibers in 0^o ply is found at bearing damage zone, while, it is found at net-tension damage zone for 90^o ply. The same observation is found for tensile failure of fibers but in the opposite sites.

4- In the case of net-tension failure mode, the largest size of fiber tension damage zone is found in 0^o ply.

5- Hashin failure criteria associated with delamination damage approach is a good candidate to predict the failure stages of composite pinned joint.

6- Load-pin displacement curves predicted by Hashin associated with delamination model are more closed to experimental curves than those predicted by Hashin model only.

7- For *W/D* = 2 and 3, a brittle failure (net-tension) of composite pinned joint is observed, while, for *W/D* = 4 and 5, a ductile failure (bearing followed by shear-out) of composite pinned joint is observed.

Acknowledgements

This research was supported by the Deanship of Scientific Research (DSR) at Jazan University, KSA. Project: DSR # JUP7/069/2017.

References

ABAQUS analysis user's manual. (2016). Version 2016. Dassault Systèmes.

Abd-Elhady, A. and Sallam, H.E.M. (2015). Crack sensitivity of bolted metallic and polymeric joints, Engineering Fracture Mechanics 147:55–71.

Barbero E.J., Cosso F.A., Roman R., Weadon T.L. (2013). Determination of Material Parameters for Abaqus Progressive Damage Analysis of E-Glass Epoxy Laminates, Composite Part B, 46:211-220.

Benzeggagh, M., Kenane, M. (1996). Measurement of mixed-mode delamination fracture toughness of unidirectional glass/epoxy composites with mixed mode bending apparatus. Compos Sci Technol, 56: 439–49.

El-Emam, H.M., Salim, H., and Sallam, H.E.M. (2016). Composite patch configuration and prestraining effect on crack tip deformation and plastic zone for inclined cracks. J. Compos. Constr. 20(4), DOI:10.1061/(ASCE)CC.1943-5614.0000655, 04016002.

El-Emam, H.M., Salim, H., and Sallam, H.E.M. (2017). Composite patch configuration and prestress effect on SIFs for inclined cracks in steel plates, J. Struct. Eng. 143(5), DOI: 10.1061/(ASCE)ST.1943-541X.0001727.

El-Sisi, A.E., Salim, H.A., El-Hussieny, O.M., Sallam, H.E.M. (2014). Behaviors of a cracked lapped joint under mixed mode loading, Engineering Failure Analysis 36: 134–146.

El-Sisi, A.E., El-Emam, H.M., Salim, H.A., Sallam, H.E.M. (2015). Efficient 3D modeling of damage in composite materials. Journal of Composite Materials 49: 817-828.

Ghanem, M., Al-Shorbagy, A.E., Khashaba, U. A. and Sallam, H.E.M.: Mechanical behavior and failure mode of bolted joints in polymeric composite materials. MEATIP4, Fourth Assiut University Int. Conf., December 12-14, CD-Room, Paper N0. MD06, (2006).

Hashin, Z. (1980). Failure criteria for unidirectional fiber composite, J Appl Mech 47:329–334.

Hashin Z, Rotem A. (1973). A fatigue failure criterion for fiber reinforced materials. J Compos Mater 7:448–64.

Khashaba U.A., Sallam H.E.M., Al-Shorbagy A.E., Seif M.A. (2006). Effect of washer size and tightening torque on the performance of bolted joints in composite structures, Composite Structures 73:310–317.

Krueger, R. (2004). Virtual crack closure technique: History, approach, and applications. Applied Mechanics Reviews 57:109–143

Liu, P.F., Hou, S.J., Chu, J.K., Hu, X.Y., Zhou, C.L, Liu, Y.L., Zheng, J.Y., Zhao, A., Yan, L. (2011). Finite element analysis of postbuckling and delamination of composite laminates using virtual crack closure technique. Composite Structures 93: 1549–1560.

McCarthy CT, McCarthy MA, Lawlor VP. (2005): Progressive damage analysis of multi-bolt composite joints with variable bolt–hole clearances. Composites: Part B 36:290–305.

Nassar S, Virupaksha VL, Ganeshmurthy S. (2007). Effect of bolt tightness on the behaviour of composite joints. J Pressure Vessel Technol 129:43–51.

Sallam H.E.M., Abd-Elhady A.A. (2015). Prediction of Crack Initiation Site in Fastener Hole of Composite Laminate. In: Sano T., Srivatsan T.S. (eds) Advanced Composites for Aerospace, Marine, and Land Applications II. (2015) Chapter 14, 187-198, Springer.

Sallam, H.E.M., El-Sisi, A.E., Matar, E.B., El-Hussieny, O.M. (2011). Effect of clamping force and friction coefficient on stress intensity factor of cracked lapped joints, Engineering Failure Analysis 18: 1550–1558

Warren, K.C., Lopez-Anido, R.A., Vel, S.S., Bayraktar, H.H. (2016). Progressive failure analysis of three-dimensional woven carbon composites in single-bolt, double-shear bearing. Composites Part B 84: 266-276.

Xie, D., Biggers Jr, S. B. (2006). Progressive crack growth analysis using interface element based on the virtual crack closure technique. Finite Elements in Analysis and Design, 42: 977 – 984.

Zeng, C., Tian, W., Liao, W.H. (2016). The effect of residual stress due to interference fit on the fatigue behavior of a fastener hole with edge cracks. Engineering Failure Analysis, 66: 72–87.

Zhou, Y, Lu, Z, Yang, Z. (2013). Progressive damage analysis and strength prediction of 2D plain weave composites. Compos Part B Eng 47: 220-229.